Article

Cell Reports

Vascular Endothelial Growth Factor Receptor 3 Controls Neural Stem Cell Activation in Mice and Humans

Graphical Abstract

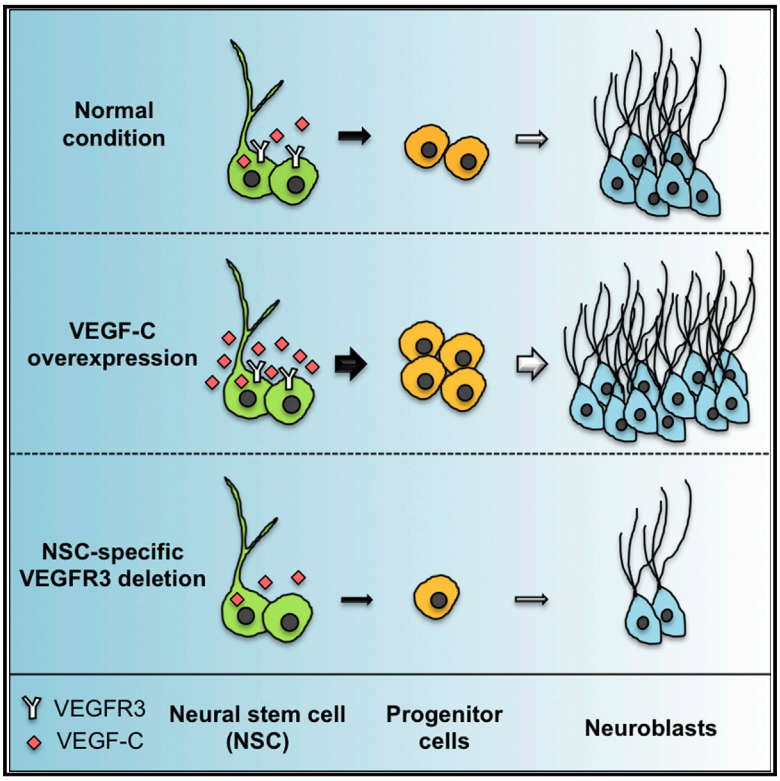

Authors

Jinah Han, Charles-Félix Calvo, ..., Anne C. Eichmann, Jean-Léon Thomas

Correspondence

anne.eichmann@yale.edu (A.C.E.), jean-leon.thomas@yale.edu (J.-L.T.)

In Brief

The mechanisms regulating neural stem cell activation in vivo are poorly understood. Han et al. show that, in the adult mouse hippocampus, neural stem cells require VEGF-C/VEGFR3 signaling to enter the cell cycle and convert into progenitor cells. The role of VEGFR3 signaling is conserved in human neural stem cells.

Highlights

- VEGFR3 is required for adult hippocampal neurogenesis
- VEGFR3 signaling converts quiescent neural stem cells into progenitor cells
- VEGF-C/VEGFR3 activates human neural stem cells through ERK and AKT

Accession Numbers

GSE55621

Han et al., 2015, Cell Reports *10*, 1158–1172
February 24, 2015
http://dx.doi.org/10.1016/j.celrep.2015.01.049

CellPress

OPEN ACCESS
CellPress

Cell Reports
Article

Vascular Endothelial Growth Factor Receptor 3 Controls Neural Stem Cell Activation in Mice and Humans

Jinah Han,[1] Charles-Félix Calvo,[2,3,4] Tae Hyuk Kang,[5] Kasey L. Baker,[1] June-Hee Park,[5] Carlos Parras,[2,3,4] Marine Levittas,[2,3,4] Ulrick Birba,[2,3,4] Laurence Pibouin-Fragner,[1] Pascal Fragner,[1] Kaya Bilguvar,[6] Ronald S. Duman,[7] Harri Nurmi,[8] Kari Alitalo,[8] Anne C. Eichmann,[1,*] and Jean-Léon Thomas[2,3,4,5,*]

[1]Yale Cardiovascular Research Center, Section of Cardiovascular Medicine, Department of Internal Medicine, Yale University School of Medicine, New Haven, CT 06510-3221, USA
[2]Université Pierre and Marie Curie–Paris 6
[3]INSERM/CNRS U-1127/UMR-7225
[4]APHP
Groupe Hospitalier Pitié-Salpètrière, 75013 Paris, France
[5]Department of Neurology
[6]Department of Genetics
[7]Department of Psychiatry
Yale University School of Medicine, New Haven, CT 06510-3221, USA
[8]Wihuri Research Institute and Translational Cancer Biology Program, Biomedicum Helsinki, University of Helsinki, 00014 Helsinki, Finland
*Correspondence: anne.eichmann@yale.edu (A.C.E.), jean-leon.thomas@yale.edu (J.-L.T.)
http://dx.doi.org/10.1016/j.celrep.2015.01.049

SUMMARY

Neural stem cells (NSCs) continuously produce new neurons within the adult mammalian hippocampus. NSCs are typically quiescent but activated to self-renew or differentiate into neural progenitor cells. The molecular mechanisms of NSC activation remain poorly understood. Here, we show that adult hippocampal NSCs express vascular endothelial growth factor receptor (VEGFR) 3 and its ligand VEGF-C, which activates quiescent NSCs to enter the cell cycle and generate progenitor cells. Hippocampal NSC activation and neurogenesis are impaired by conditional deletion of *Vegfr3* in NSCs. Functionally, this is associated with compromised NSC activation in response to VEGF-C and physical activity. In NSCs derived from human embryonic stem cells (hESCs), VEGF-C/VEGFR3 mediates intracellular activation of AKT and ERK pathways that control cell fate and proliferation. These findings identify VEGF-C/VEGFR3 signaling as a specific regulator of NSC activation and neurogenesis in mammals.

INTRODUCTION

The adult mammalian brain continuously produces new neurons in two discrete regions, the subventricular zone (SVZ) lining the ventricles and the dentate gyrus (DG) of the hippocampus (Altman and Das, 1965; Doetsch et al., 1999). In rodents, hippocampal neurogenesis is enhanced by external factors, including an enriched environment and voluntary running exercise (Brown et al., 2003; Vivar and van Praag, 2013). A decline in hippocampal neurogenesis occurs with age and may underlie cognitive and mood alterations associated with aging and Alzheimer's disease (Lazarov et al., 2010; Mu and Gage, 2011).

Hippocampal neurogenesis occurs within the subgranular zone (SGZ) of the DG and is initiated by neural stem cells (NSCs), which undergo a series of divisions to generate new granular layer interneurons that integrate into the hippocampal circuitry (Kempermann et al., 2004). NSCs include a quiescent population, which are radial glia-like cells (RGLs) (or type-1 cells) that are characterized by the expression of Nestin, GFAP, Sox2, and Hes5 (Bonaguidi et al., 2011; Encinas et al., 2011; Lugert et al., 2010; Suh et al., 2007). NSC activation is upon Ascl1 regulation (Andersen et al., 2014) and leads to generate proliferative progenitors, known as intermediate progenitors (IPCs), which in turn give rise to committed neuronal progenitors (neuroblasts). Whereas the steps of hippocampal neuron formation have been well characterized (Bonaguidi et al., 2012; Kempermann et al., 2004), the molecular mechanisms controlling this cellular progression remain poorly understood.

Several signaling pathways are known to maintain hippocampal NSC quiescence through inhibition of cell proliferation. Conditional disruption of the genes encoding BMP2 and 4, sFRP3, Notch/RBP-J, and REST in RGLs all result in rapid activation of NSC division, leading to a transient increase in IPC numbers and production of new adult hippocampal neurons (Ehm et al., 2010; Gao et al., 2011; Jang et al., 2013; Mira et al., 2010). In contrast to these repressors of NSC activation, only a few positive regulators of NSC division and progenitor cell production are known. These include sonic hedgehog/smoothened and BDNF/TrkB, but both of these

signaling pathways are also active in other subpopulations of the hippocampal niche (Li et al., 2008; Machold et al., 2003). Identification of NSC-selective positive regulators should allow prolonging or enhancing neurogenesis during aging and improve the efficacy of NSC-based repair therapies, especially in older patients.

Vascular endothelial growth factors (VEGFs) and their high-affinity tyrosine kinase receptors (VEGFRs) are potent regulators of the growth and maintenance of vascular and neural cells (Eichmann and Thomas, 2013; Zacchigna et al., 2008). In the hippocampus, VEGF-A increases angiogenesis, neurogenesis, and neuronal plasticity (During and Cao, 2006; Fournier and Duman, 2012; Licht and Keshet, 2013). However, it is not clear whether VEGF-A enhances neurogenesis directly, through its receptors VEGFR1 and 2 on neural cells, or indirectly, through factors released from newly formed blood vessels. The related growth factor VEGF-C is a potent regulator of lymphangiogenesis (Lohela et al., 2009). VEGF-C also induces angiogenesis but only weakly, as expression of its receptor VEGFR3 is mainly restricted to tip cells at the extremities of growing blood vessels (Tammela et al., 2008). In the brain, we have previously shown that VEGF-C stimulates neurogenesis via direct cell-autonomous actions of VEGFR3 in neural cells. Deletion of *Vegf-c* impairs neural development in both *Xenopus* and mouse embryonic brains, and conditional deletion of *Vegfr3* within NSCs affects neurogenesis in the adult mouse SVZ (Calvo et al., 2011; Le Bras et al., 2006). We hypothesized that VEGF-C-VEGFR3 signaling might affect hippocampal NSCs in mice and humans, thereby controlling neurogenesis.

Here, we examined the role of VEGFR3 and its mechanism of action in adult hippocampal NSCs. We show that the VEGF-C/VEGFR3 pathway is a positive signal that selectively promotes NSC activation and conversion into progenitor cells in mice. Moreover, VEGFR3 signaling is conserved in human NSCs where VEGF-C activates ERK- and AKT-signaling pathways. Taken together, these data identify VEGF-C/VEGFR3 as a novel signaling pathway in mammalian NSCs that may be targeted therapeutically to improve neurogenesis.

RESULTS

Vegfr3 and *Vegf-c* Expression in the Hippocampal DG

We characterized the expression of *Vegfr3* in the adult hippocampus using *Vegfr3*::*YFP* BAC-transgenic mice (Calvo et al., 2011). YFP labeled capillaries and neural cells localized along the SGZ (Figure 1A). Flow cytometric analysis of dissociated DG cells confirmed that 16% of neural cells ($CD31^-$ non-endothelial cells) were YFP-expressing cells, hereafter referred to as $Vegfr3^{YFP}$ cells (Figures 1B and S1A). Quantitative RT-PCR (qRT-PCR) showed that *Vegfr3* transcripts are highly enriched in $Vegfr3^{YFP}$ cells compared to DG neural cells, whereas lower levels of the two other VEGFR family members *Vegfr1* and *Vegfr2* were found in $Vegfr3^{YFP}$ cells (Figures 1C and S1B). qRT-PCR also showed enrichment of ligand *Vegf-c* transcripts in $Vegfr3^{YFP}$ cells, suggesting possible autocrine VEGF-C/VEGFR3 signaling in these cells (Figure S1B). In addition, prominent VEGF-C expression was seen in DG cells surrounding the SGZ by X-gal staining of $Vegfc^{LacZ+}$ knockin mice and antibody staining (Figures 1D and 1E), indicative of possible paracrine VEGF-C signaling to $Vegfr3^{YFP}$ cells.

To examine whether this ligand-receptor system functioned in hippocampal neurogenesis, we determined which type of neural cells expressed VEGFR3. About half of $Vegfr3^{YFP}$ cells (55%) exhibited a RGL morphology characteristic of NSCs (type-1a) and stained positive for GFAP, Nestin, or BLBP radial glia markers (Figures 1F–1H and S1C). Almost all $Vegfr3^{YFP}$ RGL cells expressed GFAP (99%), including a 17% subpopulation that lacked Nestin expression. Previous reports showed that $GFAP^+/Nestin^-$ RGL cells are quiescent NSCs and suggested that $GFAP^+/Nestin^+$ RGL cells are activated NSCs (DeCarolis et al., 2013), which would indicate that $Vegfr3^{YFP}$ RGL cells include both quiescent and activated NSCs. The other 45% of $Vegfr3^{YFP}$ cells lacked radial processes (Figure 1G). Less than 10% of those cells exhibited weaker YFP and stained for the IPC markers Ascl1 and Tbr2, and the rest included $S100\beta^+$ astrocytes (15%) and non-radial $Tbr2^-$ cells that may correspond to non-radial NSCs (20%). DCX^+ neuroblasts as well as postmitotic interneurons were excluded from the $Vegfr3^{YFP}$ population (Figures 1F, 1H, and S1C). Flow cytometric analysis of $Vegfr3^{YFP}$ cells confirmed that they include a majority of $S100\beta^+/Glast^+/GFAP^+$ astroglial cells (65%–70%) and $Sox2^+$ (50%) cells (Figure S1D; Table S1). RNA-sequencing analysis (RNA-seq) also showed enrichment of transcripts encoding NSPC markers in $Vegfr3^{YFP}$ cells, and specific expression of *GFAP*, *Nestin*, *Blbp*, *Ascl1*, *Tbr2*, and *Sox2* in $Vegfr3^{YFP}$ cells was confirmed by qRT-PCR and flow cytometric analysis (Figures S1E and S2A; Table S2).

Analysis of proliferation showed that $Vegfr3^{YFP}$ RGL cells are mainly quiescent ($Ki67^-$) whereas non-radial $Vegfr3^{YFP}$ cells include a few dividing cells (5% $Ki67^+$; Figure 1I). Following a short BrdU-pulse (3 hr) to label proliferating NSCs and IPCs, 60% of $BrdU^+$ cells were $Vegfr3^{YFP}$ cells (Figures 1J and 1K). Altogether, these data show that *Vegfr3* expression characterizes NSCs and declines in neural progenitor cells in the adult hippocampal SGZ (Figure 1L).

VEGF-C/VEGFR3 Signaling Activates Hippocampal NSCs In Vitro

To test the stem cell properties of $Vegfr3^{YFP}$ cells, we sorted $Vegfr3^{YFP}$ and $Vegfr3^{YFP\text{-}negative}$ DG cells and analyzed their ability to form neurospheres, self-renew, and differentiate into neural cell types in vitro (Figure 2). We found that neurospheres formed exclusively from $Vegfr3^{YFP}$ cells, but not from the fraction of $Vegfr3^{YFP\text{-}negative}$ cells, which establishes that $Vegfr3^{YFP}$ cells are NSCs (Figure 2A). Neurospheres derived from $Vegfr3^{YFP}$ cells were able to self-renew for at least six passages, confirming the presence of NSCs with *long-term* self-renewal capacity (Figure 2B). $Vegfr3^{YFP}$ neurosphere cells transferred onto Matrigel differentiated into $Tuj1^+$ neurons (13%) and $GFAP^+$ astrocytes (71%) but rarely into $O4^+$ oligodendrocytes (0.9%), which is consistent with previous reports showing that DG NSCs generate only very few oligodendroglial cells (Bonaguidi et al., 2011; Figure 2C). $Vegfr3^{YFP}$ cells are therefore NSCs, which maintain self-renewal and multilineage differentiation capacities.

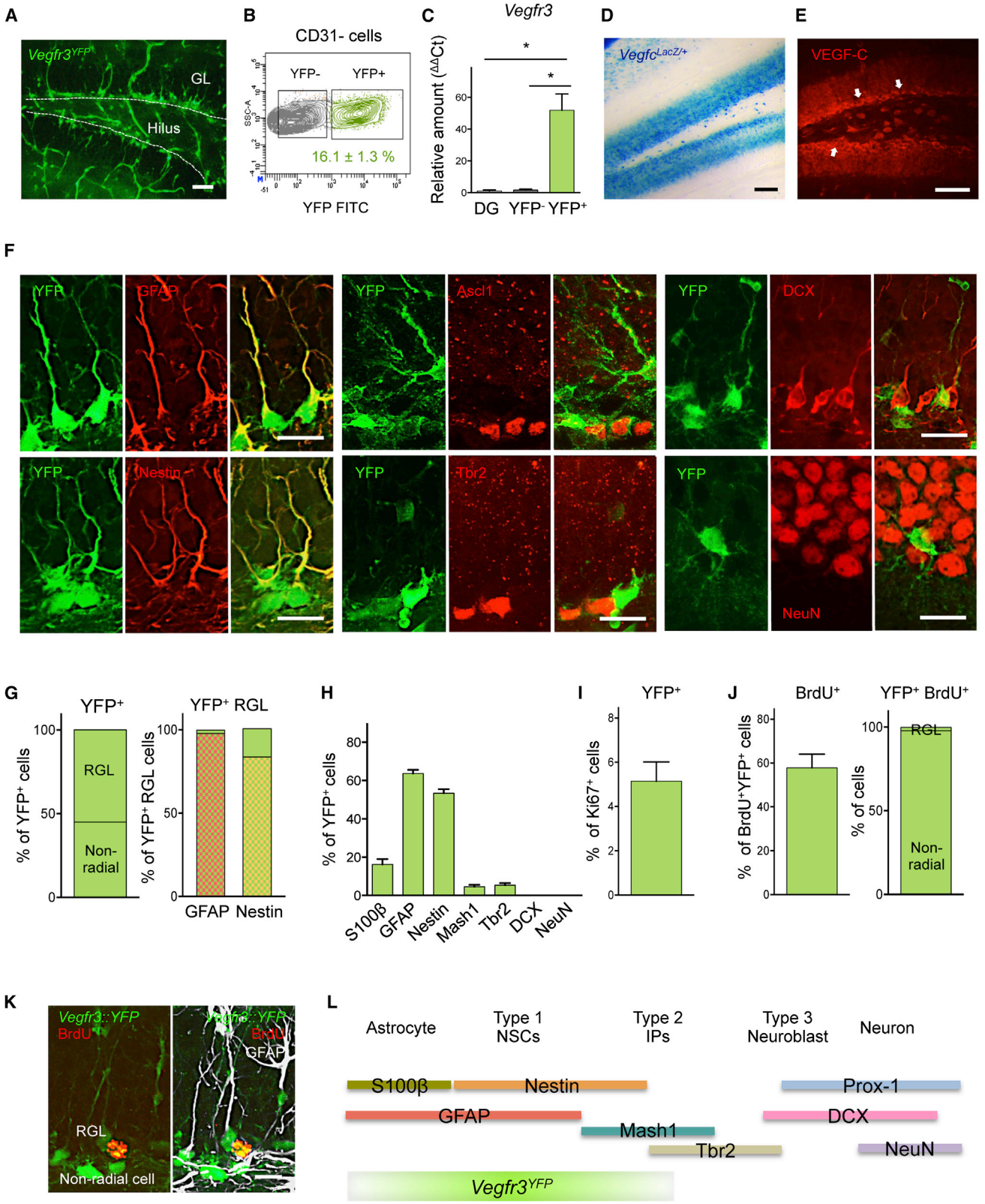

(legend on next page)

Addition of recombinant VEGF-C (50 ng/ml) had no effect on cell survival (Figure 2D). However, VEGF-C-stimulated *Vegfr3*^{YFP} cells generated more neurospheres (Figure 2E). The activation of *Vegfr3*^{YFP} cells by VEGF-C was blocked by treatment with a blocking antibody against VEGFR3 (31C1), indicating that the response to VEGF-C is VEGFR3 dependent (Figure 2E).

To get a molecular readout of VEGF-C action on hippocampal NSCs, we performed RNA-seq. As shown in Figure S2B and Table S2B, VEGF-C-treated *Vegfr3*^{YFP} cells, but not *Vegfr3*$^{YFP\text{-}negative}$ cells, strongly upregulated mRNA expression of regulators of the G1-S transition, such as cyclin D/E and cyclin-dependent kinases Cdk1/2, and of factors regulating chromosomal DNA replication. Furthermore, VEGF-C stimulation appears to drive NSCs from their quiescent state toward a proliferating progenitor state. In VEGF-C-treated cells, the expression of NSC markers such as Notch1/2 (Ables et al., 2010), Hes5 (Imayoshi et al., 2013), Ctnnb1(β1-catenin) (Lie et al., 2005), Bmpr1 (bone morphogenetic protein receptor) (Mira et al., 2010), Mhi1/2 (Mushashi1/2) (Okano et al., 2005), Bmi-1 (Fasano et al., 2009), and Rest (Abrajano et al., 2010) are downregulated whereas the expression of progenitor cell markers Ascl1 (Kim et al., 2008; Lugert et al., 2012), Sox21 (Matsuda et al., 2012), and Numb (Aguirre et al., 2010; Petersen et al., 2002) are upregulated (Figure S2B; Table S2B). To confirm the effect of VEGF-C on cell cycle progression, we analyzed the cell cycle activity of *Vegfr3*^{YFP} cells. After overnight culture in the presence or absence of VEGF-C, cells were stained with *Pyronin Y*/ *Hoechst* 33342 and analyzed by flow cytometry (Figure 2F). VEGF-C treatment of *Vegfr3*^{YFP} cells, but not of *Vegfr3*$^{YFP\text{-}negative}$ cells, promotes a significant increase of cells *in G1 phase* (Figure 2F). Taken together, these data demonstrate that VEGF-C/VEGFR3 signaling in NSCs initiates cell cycle entry and conversion of quiescent cells into proliferating progenitor cells.

Maintenance of Hippocampal Neurogenesis In Vivo Requires VEGFR3

We next investigated consequences of inducible *Vegfr3* deletion in hippocampal NSCs in vivo, using *Glast*^{CreERT2} to delete *Vegfr3*$^{flox/flox}$ allele (*Glast i⊿R3*) (Figures 3 and S3). The *Glast*^{CreERT2} driver line allows the targeting of Glast$^+$ NSCs that express *Vegfr3.* Restricted expression of Glast in glial cells excluded non-radial progenitor cells in the DG (Figure S3A; DeCarolis et al., 2013; Mori et al., 2006). Mice were sacrificed 1 or 5 months after Tx treatment to test the effects of *Vegfr3* deletion in neurogenesis. Intercross of *Glast*^{CreERT2} mice with ROSA26 and mT/mG reporter lines led to genetic recombination in >65% of SGZ cells, indicating that *Glast*^{CreERT2} likely drove mosaic deletion of *Vegfr3* in hippocampal NSCs (Figures S3A and S3B). Genetic recombination of *Vegfr3* locus was assessed by PCR in Tx-treated *Glast i⊿R3* mice (Figure S3C). *Glast i⊿R3* and control (*Vegfr3*$^{flox/flox}$) animals were given a 3 hr BrdU pulse prior to sacrifice to label activated NSCs (Figure 3A). One-month Tx-*Glast i⊿R3* and control mice showed similar numbers of BrdU$^+$ SGZ cells and DCX$^+$ neuroblasts (Figures 3B–3E). This result was expected because *Vegfr3* deletion occurs in Glast$^+$ NSCs that rarely divide and slowly differentiate into DCX$^+$ cells (DeCarolis et al., 2013). In contrast, 5-month Tx-*Glast i⊿R3* mice showed a 40% decrease in the number of BrdU$^+$ NSCs and DCX$^+$ neuroblasts compared to controls (Figures 3B–3E). The number of GFAP$^+$Nestin$^+$ RGL cells and of astrocytes in the hilus was similar between controls and *Glast i⊿R3* mice (Figures 3F and 3G). The number of RGL cells was also not altered in *Glast i⊿R3*; *Vegfr3*::*YFP* mice expressing YFP in RGL cells (Figure S3D). Altogether, these data indicate that decline of hippocampal neurogenesis in *Glast i⊿R3* is not caused by a primary loss of NSCs or by an abnormal neuron/astrocyte differentiation balance. Anti-active caspase 3 antibody labeling and TUNEL staining of the DG showed only rare cells engaged in programmed cell death (PCD) in both Tx-control and -*Glast i⊿R3* mice, indicating that *Vegfr3* deletion did not induce PCD in DG cells (data not shown). Therefore, *Vegfr3* loss of function in NSCs does not compromise NSC survival and renewal but selectively impairs NSC activation and conversion into proliferative IPCs.

Decline of hippocampal neurogenesis is associated with cognitive impairments and an enhancement of fear and anxiety in both mice and humans (Encinas and Sierra, 2012; van

Figure 1. *Vegf-c/Vegfr3* Are Expressed by Adult Hippocampal Stem Cells

(A) Coronal DG section of an adult *Vegfr3*::*YFP* mouse. YFP expression is detected both in vessels and SGZ cells. White dotted line indicates SGZ.

(B) Isolation of *Vegfr3*^{YFP} cells from the DG of adult *Vegfr3*::*YFP* mice. After exclusion of CD31$^+$ endothelial cells, a subset of *Vegfr3*^{YFP} cells were sorted by FACS.

(C) qRT-PCR analysis of FACS-sorted cells from the DG of *Vegfr3*::*YFP* adult mice. *Vegfr3* transcripts are specifically enriched in *Vegfr3*^{YFP} cells compared to total DG neural cells (non-endothelial DG cells) and *Vegfr3*$^{YFP\text{-}negative}$ cells. n = 3 independent experiments; bars: mean ± SEM; Student's t test: $p < 0.05$ (*).

(D and E) Coronal DG section of adult *Vegfc*$^{lacZ/+}$ mouse stained with X-gal and of wild-type mouse labeled with anti-VEGF-C Ab (E). White arrows indicate a higher level of VEGF-C expression in SGZ.

(F) Representative images of coronal DG sections in adult *Vegfr3*::*YFP* mice stained with Abs against markers of RGL (GFAP and Nestin), progenitor cells (Ascl1 and Tbr2), neuroblasts (DCX), and neurons (NeuN) (red).

(G) Quantification of *Vegfr3*^{YFP} SGZ cells by their morphology. Percentage of *Vegfr3*^{YFP} RGL cells expressing GFAP and Nestin.

(H) Quantification of *Vegfr3*^{YFP} SGZ cell subtypes according to their antigen expression. y axis: % of YFP$^+$ marker$^+$ cells/YFP$^+$ cells. Total 30–500 cells were counted from three to six sections.

(I) 5% of *Vegfr3*^{YFP} SGZ cells has entered the cell cycle (Ki67$^+$). n = 100–150 cells/section, counted from seven sections. Bars: mean ± SEM.

(J) *Vegfr3*^{YFP} cells represent 60% of BrdU$^+$ SGZ cells. Most BrdU$^+$ *Vegfr3*^{YFP} cells are non-radial cells (98%), and only a few of them are RGL cells (2%). n = 30–50 cells counted from five sections.

(K) *Vegfr3*^{YFP} SGZ cell morphology and activity. An anti-GFAP Ab labels RGLs (white), but not YFP$^+$-non-radial cells. A 3-hr pulse of BrdU (red) labels exclusively non-radial YFP$^+$ cells.

(L) Comparison of the expression of *Vegfr3*^{YFP} and other stage-specific markers in SGZ cells. *Vegfr3*^{YFP} expression is specific to NSCs and progenitor cells.

The scale bars represent 100 μm (A, D, and E) and 16 μm (F and K).

See also Figure S1.

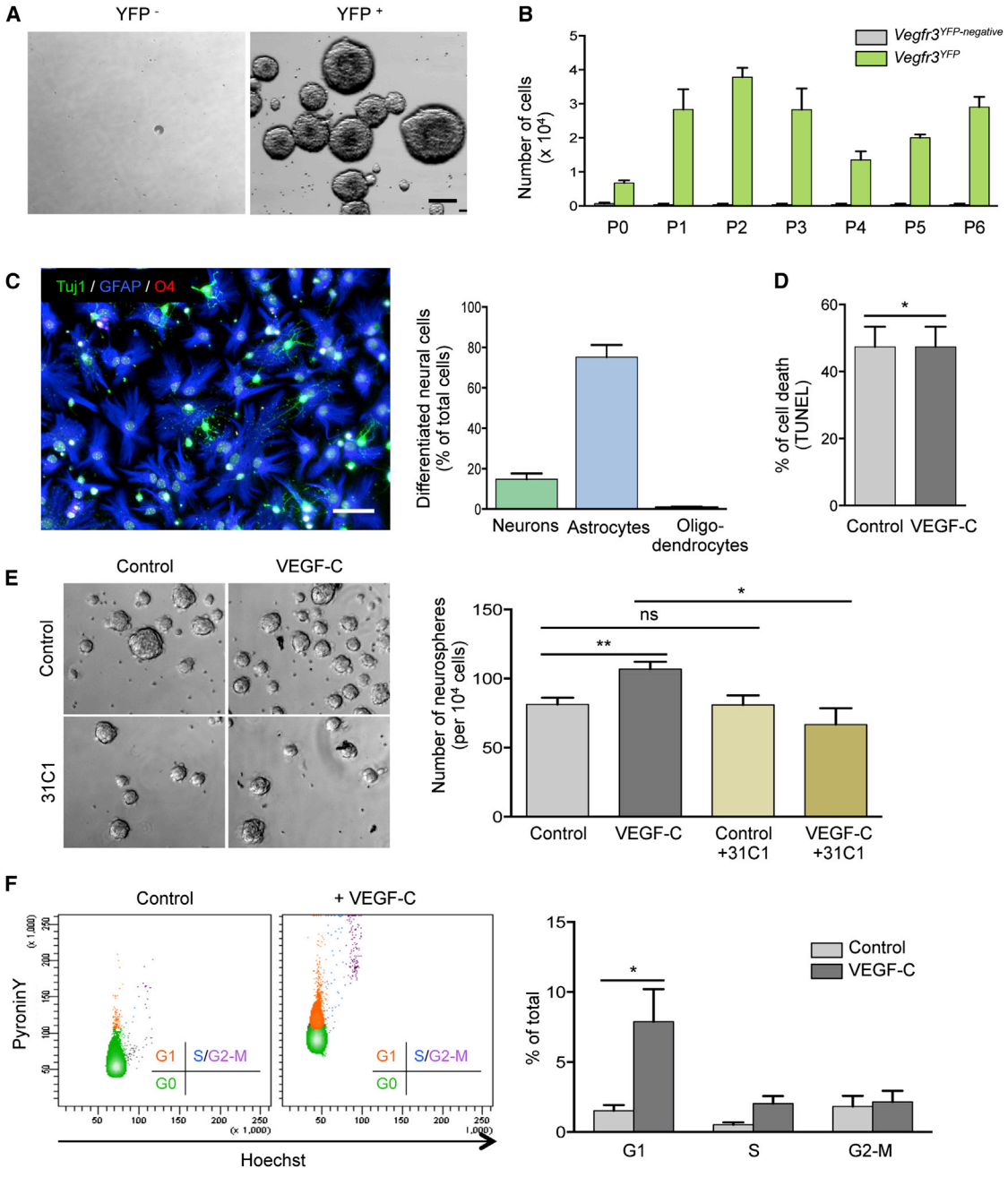

Figure 2. VEGF-C/VEGFR3 Signaling Activates Hippocampal NSCs In Vitro

(A and B) Neurosphere cultures derived from sorted *Vegfr3*^{YFP} and *Vegfr3*$^{YFP\text{-negative}}$ cells. The formation of neurospheres was only observed in *Vegfr3*^{YFP} cell cultures that can self-renew for at least six successive passages.

(C) Representative images and quantification of neurosphere differentiation. *Vegfr3*^{YFP} cells differentiate into TuJ1^{+} neuron (green), GFAP^{+} astrocyte (blue), and very few O4^{+} oligodendrocyte (red).

(D) Cell death was quantified by TUNEL staining.

(E) Representative images and quantification of neurospheres after treatment with VEGF-C (50 ng/ml) and a VEGFR3-function-blocking antibody (31C1).

(F) FACS profile and cell cycle analysis of control *Vegfr3*^{YFP} cells and VEGF-C-treated *Vegfr3*^{YFP} cells after *Pyronin Y*/*Hoechst* 33342 staining.

The scale bars represent 50 μm (A and C).

Student's t test: $p < 0.05$ (*); $p < 0.005$ (**); not significant (ns). Bars: mean ± SEM; n = 3–5 independent experiments.

See also Figure S2.

Wijngaarden and Franklin, 2013). We reasoned that decreased neurogenesis in 5-month Tx-*Glast iΔR3* mice might lead to behavioral defects. Five-month Tx-*Glast iΔR3* and -age-matched control mice were subjected to two paradigms to assess anxiety and locomotor activity: the elevated plus maze (EPM) test (Pellow et al., 1985) and the open-field (OF) test (Gould et al., 2009), respectively (Figures 3H, 3I, and S3E–S3K). Five-month Tx-*Glast iΔR3* mice displayed an anxiety phenotype in the EPM task, which was not due to a change in locomotor activity (Figures 3H, 3I, and S3E–S3K). Altogether, these results suggest a VEGFR3-dependent correlation between the decline of hippocampal neurogenesis and an increase of fear/anxiety status that manifests in middle-aged mice.

VEGF-C/VEGFR3 Signaling Activates Hippocampal NSCs In Vivo

Because VEGF-C treatment drives NSC cell cycle entry in vitro, we investigated whether VEGF-C/VEGFR3 signaling also promoted NSC activation in vivo. VEGF-C was overexpressed during 2 to 3 weeks within the hippocampus of C57BL/6 adult mice by stereotaxic injection of adeno-associated virus (AAV) encoding full-length VEGF-C (AAV-VEGF-C) above the DG (Figure 4A). AAV-EGFP was used as a control, and GFP expression in the hippocampal region showed that all animals had been efficiently infected (Figure S4A). VEGF-C induced a 2-fold increase in the number of $BrdU^+$ SGZ cells compared to control (Figure 4B). Consequently, the number of hippocampal DCX^+ cells was increased, as shown at 5 weeks after AAV-VEGF-C injection (Figure 4C). No changes in the density of DG capillaries were observed in AAV-VEGF-C-treated compared to control animals (Figures S4B and S4C). The effect of VEGF-C on NSC activation is therefore unlikely to be a secondary consequence of angiogenesis.

To determine whether VEGF-C acted specifically on $Vegfr3^{YFP}$ SGZ cells, AAV-VEGF-C was administered to adult *Vegfr3::YFP* mice. Two weeks following AAV-VEGF-C infection, $BrdU^+$ $Vegfr3^{YFP}$ cells increased around 60% in number compared to AAV-EGFP-injected controls (Figures 4D and 4E). Especially, the number of $BrdU^+$ $Vegfr3^{YFP}$ RGL cells increased in AAV-VEGF-C-treated mice, suggesting that VEGF-C targets and activates quiescent $Vegfr3^{YFP}$ NSCs (Figures 4F and 4G).

We expected that loss of *Vegfr3* function in NSCs should abolish the response to VEGF-C. AAV-VEGF-C or AAV-EGFP was delivered into the hippocampus of *Glast iΔR3* mice and controls 3 weeks after Tx injection (Figure 4H). Two weeks later, Tx-treated control mice responded robustly to AAV-VEGF-C treatment by a significant increase in the number of $BrdU^+$ NSCs. In contrast, VEGF-C overexpression failed to promote NSC proliferation in *Glast iΔR3* mice (Figures 4I and 4J). VEGFR3 is therefore required for the response of hippocampal NSCs to VEGF-C, suggesting that VEGF-C/VEGFR3 signaling activates NSCs in vivo.

VEGFR3 Signaling Regulates Exercise-Induced Activation of Hippocampal NSCs

We asked whether VEGF-C/VEGFR3 signaling controlled the NSC response to running activity, which promotes hippocampal NSC activation. First, we characterized the response of $Vegfr3^{YFP}$ cells (Figure 5A). Running *Vegfr3::YFP* mice showed a robust increase in the number of $BrdU^+$ $Vegfr3^{YFP}$ cells compared to sedentary controls (Figure 5B). The total population of $Vegfr3^{YFP}$ cells was not increased (Figure S5A), but $BrdU^+$ $Vegfr3^{YFP}$ cells significantly increased (Figures 5B and S5B). Therefore, running activity promotes activation of $Vegfr3^{YFP}$ cells. This effect occurs in the absence of significant vascular remodeling (Figures S5C–S5E). As shown in Figure S5F, running activity had no significant effect on the level of *Vegfc* expression but increased *Vegfr3* transcript expression in the DG. *Vegfr3* expression likely amplifies in $Vegfr3^{YFP}$ cells because the number of these cells remained stable. Altogether, these data indicate that the running-activity-induced hippocampal neurogenesis involves the activation of $Vegfr3^{YFP}$ NSCs and the upregulation of *Vegfr3* expression in these cells.

To determine whether VEGFR3 was required for the exercise-induced activation of $Vegfr3^{YFP}$ NSCs, *Glast iΔR3* and control mice were housed with a running wheel for 3 weeks after Tx treatment (Figure 5C). *Glast iΔR3* mice displayed a normal running activity with similar running distance compared to control mice (Figure S5G). However, *Glast iΔR3* mice were unable to activate running-induced neurogenesis, and the number of their $BrdU^+$ SGZ cells was comparable with controls (Figures 5D and 5F). In contrast, running still increased the number of DCX^+ neuroblasts in *Glast iΔR3* mice similar to controls (Figures 5E and 5G). A possible explanation for the lack of effect on the DCX^+ cells is that the loss of NSCs in Tx-Glast iΔR3 mice might be compensated for by the increased proliferation of early neuroblasts ($Tbr2^+DCX^+$), which is known to be induced by running activity (Hodge et al., 2008). Therefore, hippocampal NSC activation in response to running activity is VEGFR3 dependent but does not affect short-term production of newborn neurons.

VEGFR3 Activates ERK- and AKT-Signaling Pathways in Human NSCs

To determine whether VEGFR3 signaling is conserved in human NSCs and to identify downstream targets of VEGFR3, we analyzed VEGFR3 expression and signaling pathways in cultures of NSCs derived from human embryonic stem cells (hESCs) (H1 and H9 cell lines). hESCs were differentiated into free-floating NSC-containing spherical neural masses (SNMs) (Figures S6A–S6C). Western blot and immunostaining analyses demonstrate that SNMs derived from either H9 or H1 hESCs express VEGFR3, but not VEGFR2 (Figures 6A, 6B, and S6D). $VEGFR3^+$ cells display elongated cytoplasmic processes that correspond mainly to BLBP-positive NSCs, but not DCX neuroblasts, under both 3D- and flat-culture conditions (Figures 6C and S6E).

hNSC treatment with VEGF-C stimulates cell division (Figure 6D). The mitotic response to VEGF-C is preceded by a rapid induction of VEGFR3 phosphorylation (Figure 6E). VEGF-C also strongly activates intracellular signals including ERK and AKT phosphorylation (Figure 6F). At a later time point (15 min), VEGF-C treatment stimulates AKT-downstream-signaling pathways including glycogen synthase kinase 3β (GSK3β) (Figure 6F). GSK3β is inhibited by pAKT and regulates cell cycle entry, cell proliferation, and cell fate (Hur and Zhou, 2010). MAZ51, an indolinone that blocks VEGFR-3 signaling (Kirkin et al., 2004), inhibits

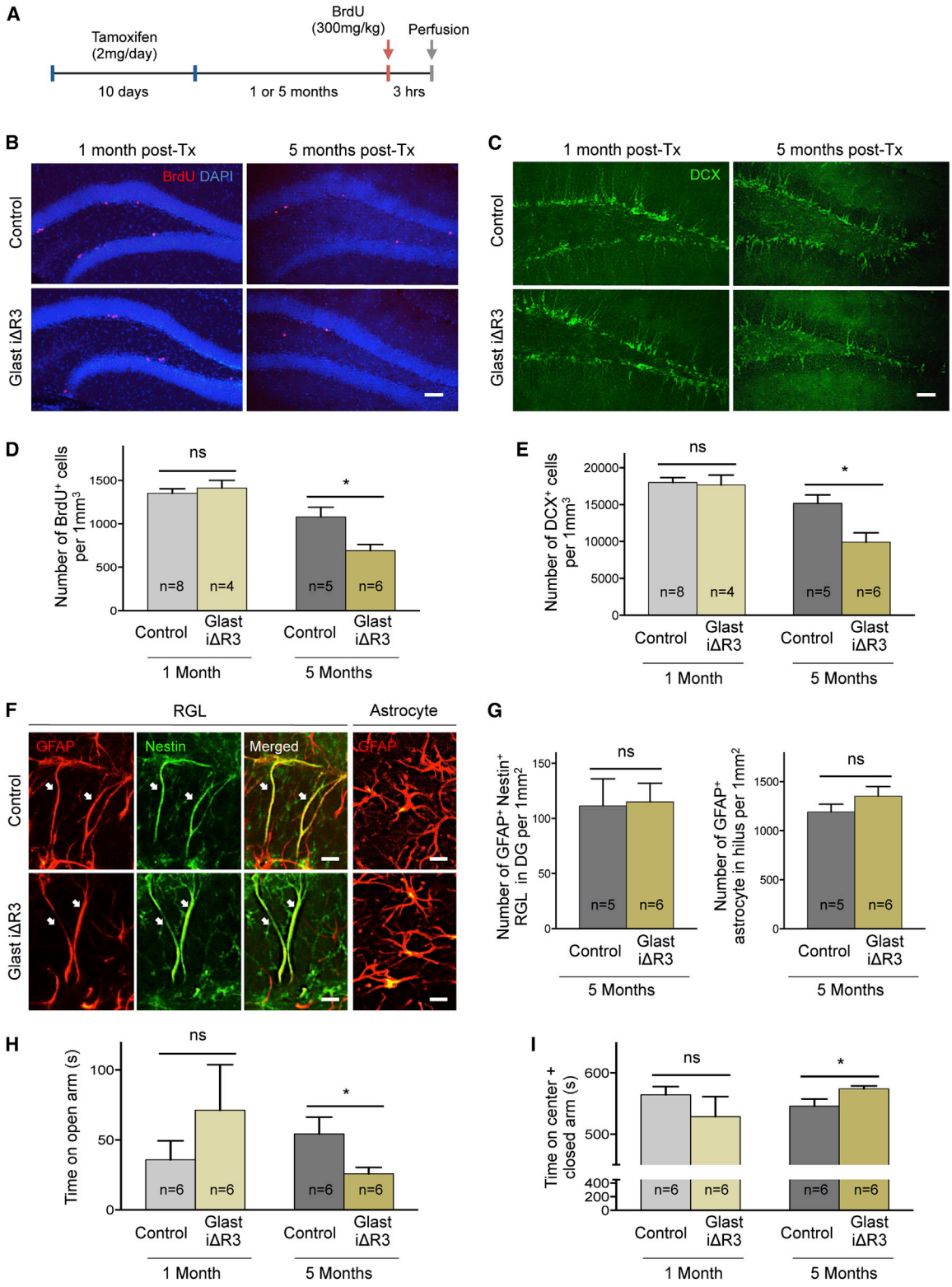

Figure 3. *Vegfr3* Deletion in Adult Hippocampal NSPCs

(A) Schedule of Tx and BrdU administration to induce *Vegfr3* deletion in NSCs and label-activated NSCs.

(B and C) Representative images of coronal DG sections from control (upper panel) and *Glast iΔR3* mice (lower panel) at indicated time points. Sections are stained for BrdU (red), DAPI (blue), and DCX (green). The scale bars represent 70 μm.

(legend continued on next page)

VEGF-C-induced AKT phosphorylation in hESC-derived NSCs (Figure S6F). Therefore, VEGF-C/VEGFR3 regulates downstream signals controlling NSC activation, providing a molecular explanation for the NSC behavioral changes observed following VEGF-C/VEGFR3 signaling manipulation.

DISCUSSION

We here identify a growth-factor-receptor-signaling pathway that promotes NSC activation during hippocampal neurogenesis. We show that *Vegfr3* is expressed by mouse hippocampal NSCs and that VEGF-C/VEGFR3 signaling is necessary for activation and conversion of NSCs into progenitor cells. Furthermore, we demonstrated that VEGF-C/VEGFR3 signaling is evolutionarily conserved in human NSCs, where it promotes cell proliferation and activates ERK/AKT pathways. To our knowledge, VEGF-C/VEGFR3 is the first known growth-factor-signaling pathway that selectively promotes NSC activation, suggesting that VEGF-C could be therapeutically used to enhance neurogenesis in humans.

We found that, like type-B astrocytes of the SVZ (Calvo et al., 2011), hippocampal NSCs exhibit *Vegfr3*^{YFP} reporter expression and a specific enrichment of *Vegfr3* transcripts. Expression of YFP in all RGL cells and the exclusive generation of neurospheres from *Vegfr3*^{YFP} DG cells strongly suggest that *Vegfr3* is characteristic for hippocampal NSCs. The *Vegfr3*::*YFP* mouse adds to the few models of transgenic reporter lines, such as *Nestin*- (Dranovsky et al., 2011; Encinas et al., 2006) and *Hes5*-reporter mice (Lugert et al., 2010), allowing the detection and sorting of adult NSCs. The level of YFP reporter expression was much higher in NSCs than progenitors, indicating that *Vegf3* is downregulated along with the asymmetric cell division of activated NSCs into progenitor cells.

Three independent lines of evidence demonstrate a direct requirement of VEGFR3 in NSC activation. First, VEGF-C treatment of *Vegfr3*^{YFP} cells, but not *Vegfr3*$^{YFP\text{-}negative}$ cells, activates cell cycle entry; second, genetic deletion of *Vegfr3* in NSCs impairs neurogenesis; and third, VEGF-C-induced NSC activation is lost in *Vegfr3* mutant mice. *Vegfr3* deletion in NSCs decreases the populations of activated NSCs and neuroblasts, without affecting the pool of NSCs in middle-aged mice. VEGFR3 activity is therefore not necessary for NSC maintenance but required for the generation of progenitors and neuroblasts, suggesting that VEGF-C/VEGFR3 signaling regulates activation of cell division in NSCs. This hypothesis is reinforced by RNA-seq data showing that VEGF-C stimulation shifts NSCs from their undifferentiated state toward a proliferating progenitor state. VEGF-C/VEGFR3 signaling in NSCs downregulates the expression of Bmi-1 and Rest, which interact with a broad array of transcriptional and epigenetic regulatory cofactors to maintain stemness and inhibit NSC differentiation (Abrajano et al., 2010; Fasano et al., 2009). This suggests that activation of VEGFR3 by VEGF-C de-represses the NSC differentiation program. VEGF-C/VEGFR3 signaling in NSCs is also characterized by upregulated expression of factors that are mandatory checkpoint regulators of the cell cycle. Although novel in the context of NSCs, this finding is not surprising when viewed from an angiogenesis perspective. VEGF-C is a well-known mitogen for VEGFR3^{+} lymphatic endothelial cells and mediates downstream signaling through activation of ERK and AKT (Koch and Claesson-Welsh, 2012), which suggests that these downstream signaling events are conserved between endothelial cells and NSCs.

The sources of VEGF-C for inducing NSC activation as well as the mechanisms regulating Vegfr3 expression in NSCs remain to be determined. NSCs contain *Vegf-c* transcripts, suggesting that, besides paracrine VEGF-C from DG cells, autocrine VEGF-C may activate VEGFR3 at the cell membrane. The discontinuous process of NSC activation also implies that VEGF-C availability may be regulated by translational or post-translational processes in NSC, perhaps through control of VEGF-C maturation by enzymes such as CCBE1 (collagen- and calcium-binding epidermal growth factor domains 1) (Le Guen et al., 2014). NSC activation is moreover likely to be controlled by a tight regulation of VEGFR3 expression levels. We found that *Vegfr3* expression in DG cells is physical activity dependent, suggesting that it could be regulated by activity-dependent epigenetic mechanisms, such as DNA methylation that modulates neurogenesis (Guo et al., 2014; Jobe et al., 2012; Saharan et al., 2013) and also controls *Vegfr3* expression in endothelial cells (Quentmeier et al., 2012). Notch signaling is another regulator that inhibits VEGFR3 expression in endothelial cells (Benedito et al., 2012), suggesting that Notch may maintain NSCs quiescence by regulating *Vegfr3* expression. Conversely, we show that VEGFR3 activation in NSCs downregulates Notch and its downstream targets, suggesting that functional antagonism between VEGFR3 and Notch could switch NSC fate from quiescence to activation. Interestingly, *Notch1* deletion in NSCs (Ables et al., 2010) induces similar phenotype to *Vegfr3* deletion in NSCs, i.e., a delayed reduction in the populations of dividing NSPCs and neuroblasts.

Another novelty of our study is the finding that VEGFR3 expression is conserved in human NSCs, where it promotes proliferation and regulates ERK and AKT, GSK3β signaling cascades in response to VEGF-C. Through VEGFR3, VEGF-C activates several downstream signaling cascades promoting transcription, such as ERK for mitogen-stimulated proliferation (Phoenix and Temple, 2010), and translation, such as mTOR and S6K signals, which regulate cell survival and cell fate decisions (Bordey, 2014; Hur and Zhou, 2010). VEGF-C is therefore able to rapidly and simultaneously regulate cell cycle entry and differentiation processes in NSCs, which likely explains its potent role in mouse hippocampal neurogenesis.

(D and E) Quantification of BrdU^{+} cells and DCX^{+} cells in the DG of control and *Glast i⊿R3* mice at 1 month and 5 months post-Tx administration.
(F and G) Representative images and quantification of RGL cells (GFAP^{+}Nestin^{+} cells in SGZ, white arrow) and astrocytes (GFAP^{+} cells in hilus) of control and *Glast i⊿R3* mice at 5 months post-Tx administration. The scale bars represent 16 μm.
(H and I) Quantification of OF and EPM test.
Student's t test: $p < 0.05$ (*); not significant (ns). Bars: mean ± SEM.
See also Figure S3.

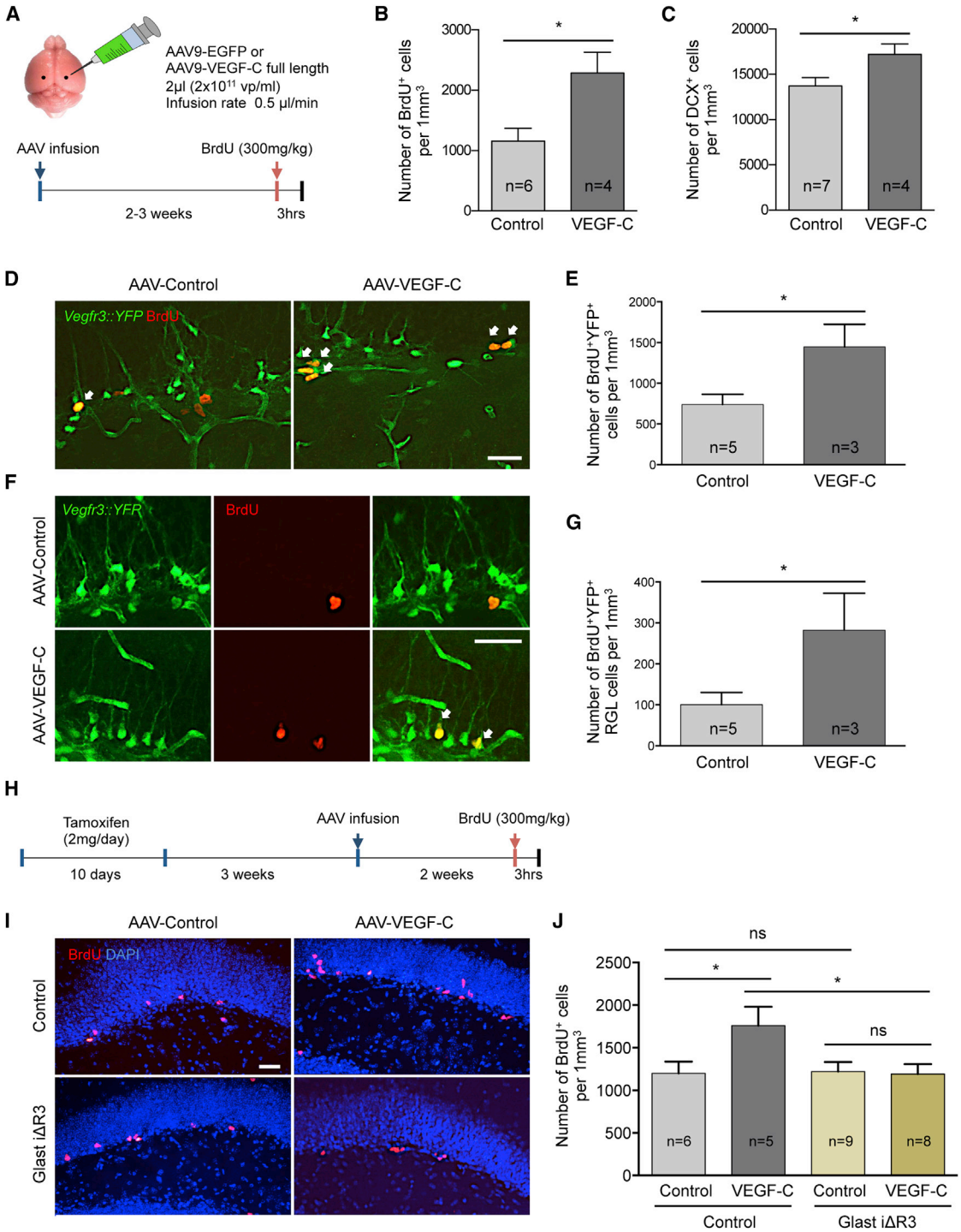

Figure 4. VEGFR3 Mediates VEGF-C-Induced Proliferation in Hippocampal NSCs

(A) Intra-hippocampal injection of AAV_9-GFP (control) and -VEGF-C. At 2 to 3 weeks after AAV infection, mice were given a 3-hr pulse of BrdU and analyzed to quantify proliferation and neuroblast production in the DG.

(B and C) Quantification of $BrdU^+$ cells and DCX^+ cells in the SGZ of control and VEGF-C-treated mice.

(D and E) Representative images and quantification of $BrdU^+Vegr3^{YFP}$ cells after VEGF-C overexpression in *Vegfr3::YFP* mice. VEGF-C treatment increases $BrdU^+Vegr3^{YFP}$ cells in SGZ (white arrows). The scale bars represent 35 µm.

(F and G) Representative images and quantification of $BrdU^+Vegr3^{YFP}$ RGL cells after VEGF-C overexpression in *Vegfr3::YFP* mice. VEGF-C treatment increases $BrdU^+Vegr3^{YFP}$ RGL cells in SGZ (white arrows). The scale bars represent 35 µm.

(legend continued on next page)

We found that, in addition to impaired neurogenesis, Tx-*Glast i⊿R3* showed increased anxiety behavior, suggesting that VEGFR3 signaling in DG NSCs may contribute to emotional response. Although further research is required to reinforce this finding, it confirms previous genetic evidence that manipulation of neurogenesis alters behavior in models of anxiety and depression (Eisch and Petrik, 2012; Gross et al., 2002; Saxe et al., 2006; Snyder et al., 2011). However, VEGFR3 is expressed by other Glast-expressing cells besides hippocampal NSCs, including tanycytes in the hypothalamic median eminence and a few astrocytes in the amygdala (Hou et al., 2011; Robins et al., 2013). These regions are involved in the regulation of the hypothalamic-pituitary-adrenal (HPA) axis that controls reactions to stress as well as mood and emotions (Canteras et al., 2010), suggesting that VEGFR3 signaling in NSC/astrocytes may act on behavior by modulating the functioning of the limbic-HPA axis.

VEGF-C can promote angiogenesis (Gaál et al., 2013) but only weakly when compared to VEGF-A, because VEGFR3-signaling activity is mainly restricted to sprouting tip cells and inhibited in other endothelial cells by Notch signaling (Tammela et al., 2011). VEGF-C may thus be a candidate factor to enhance NSC activation, without unwanted effects on other cell types. Altogether, our findings are consistent with the possibility that VEGF-C activation of NSCs could improve age-related decline in hippocampal neurogenesis and associated mood defects, such as those seen in Alzheimer's disease.

EXPERIMENTAL PROCEDURES

Animals

C57/Bl6 mice (Jackson Laboratories) were maintained in the Animal Research Center at Yale University. The *Vegfr3*::*YFP* (Calvo et al., 2011), *Glast*^{CreERT2}, *Vegfr3*$^{flox/flox}$ (Haiko et al., 2008), and *Vegf-c*$^{LacZ/+}$ (Karkkainen et al., 2004) mice have been described previously. *Glast*^{CreERT2} mice were crossed with *Vegfr3*$^{flox/flox}$ mice to generate NSC-specific and Tx-inducible *Vegfr3* mutant mice (*Glast i⊿R3*). Animals were sacrificed the days indicated in each experiment. All experiments were approved by the IACUC of Yale University.

TX Treatment

To induce genetic recombination, 2-month-old adult mice were injected intraperitoneally (i.p.) with tamoxifen (TX) once per day for 10 consecutive days (as indicated in the experiments) at a dose of 2 mg per day.

BrdU Administration

BrdU (Sigma) was administered to the adult animals via a single i.p. injection (300 mg/kg) 3 hr before sacrifice. The brains were processed for immunohistochemistry as described below.

Tissue Collection and Immunohistochemistry

Animals were anesthetized with isoflurane inhalation and perfused first with PBS and then with 4% paraformaldehyde (PFA). Brains were post-fixed overnight in 4% PFA and then washed with PBS. Brain coronal vibratome sections (40 μm) of brains were incubated with serum-free blocking solution (DAKO) for 1 hr at 4°C and then incubated overnight at 4°C with the primary Ab (listed in Table S1) diluted in PBS containing 0.1% Triton X-100 (PBST). After washing, sections were incubated with the corresponding conjugated secondary. For immunolabeling of SNMs, cryosections (20 μm) were then performed and stained as indicated above. DAPI was used for nucleus counterstaining.

β-Galactosidase Staining

Sections were immersed in 10 mM Tris-HCl (pH 7.3) containing 0.005% Na-deoxycholate, 0.01% Nonidet P40, 5 mM ferrocyanide, 5 mM ferricyanide, 2 mM $MgCl_2$, and 1 mg/ml X-gal at 37°C until the signal became visible.

Q-PCR

Vegfr3::*YFP* mice (total 108 mice) were used for FACS and further Q-PCR analysis of *Vegfr3*^{YFP} cells. RNA was isolated from sorted cells using the NucleoSpin RNA XS (Macherey-Nagel) and from tissues using RNeasy lipid tissue kit (QIAGEN). Real-time quantitative PCR reactions were performed in duplicate using the CFX-96 Real Time PCR system (Bio-Rad). Primers (Quantitect primer assays) were purchased from QIAGEN.

FACS

The DG was carefully isolated from the hippocampus; treated with papain (0.8 mg/ml; Worthington) for 30 min at 37°C; and then mechanically dissociated in PBS containing 5% FCS, 0.3% glucose, and 5 mM HEPES in order to obtain a single-cell suspension. Dissociated cells were stained with anti-CD31 Ab to exclude endothelial cells. Aria was used for sorting with the DIVA software (BD Biosciences).

Cell Cultures

FACS-sorted cells were plated at 1 × 10^4 cells/well in 24-well plates. Neurospheres were grown in Complete Culture Medium (CCM) (DMEM/F12-Glutamax [GIBCO], 20 μg/ml insulin [Sigma], 1/200 B-27 supplement [GIBCO], 1/100 N-2 supplement [GIBCO], 0.3% glucose, 5 mM HEPES, and 100 U/ml of penicillin/streptomycin) enriched with 20 ng/ml bFGF and 20 ng/ml EGF (both from Peprotech) during 10 days in vitro (DIV). To analyze cell differentiation, mechanically dissociated 10-DIV-derived neurospheres were plated onto Matrigel-coated glass coverslips in CCM without EGF/bFGF for 7 DIV. To test the effect of VEGF-C on neurosphere formation and cell survival, cells were plated in CCM containing EGF and bFGF alone or with recombinant rat VEGF-C (50 ng/ml; Reliatech) and rat 31C1- IgG2a antibodies (5 μg/ml; Imclone). Neurosphere formation was scored at 5 DIV by counting the number of neurospheres in culture. For survival assay, cells were incubated overnight on glass coverslips with or without VEGF-C (50 ng/ml), fixed, and labeled with the TUNEL detection kit (Roche 11 684 809 910).

Intra-cerebral Stereotaxic Injections

Animals were anesthetized with isoflurane, and skull holes were drilled overlying the hippocampus on both hemispheres. The site of infusion was at the following coordinates relative to bregma: anteroposterior, −1.8 mm; mediolateral, −1.8 mm; and dorsoventral, −1.8 mm. Two microliters of control AAV-EGFP (control) or AAV-VEGF-C were infused at a flow rate of 0.5 μl/min. Two to three weeks after injection, the brains were processed for immunohistochemistry as described.

Stereological Analysis

The marker (BrdU, DCX, and YFP)-positive cells were counted in a one-in-six series of five sections (40 μm, 240 mm apart) throughout the rostrocaudal extent of the dorsal DG. The sections stained with DAPI were used to measure DG area using Volocity software (PerkinElmer). The total number of marker$^+$ cells was determined by summing the number of marker$^+$ cells

(H) Schedule of Tx treatment, AAV_9 infection, and BrdU administration in control and *Glast i⊿R3* mice.
(I and J) Representative images and quantification of BrdU$^+$ SGZ cells in control (upper panel) and -*Glast i⊿R3* mice (lower panel) after VEGF-C treatment. VEGF-C overexpression increases BrdU$^+$ SGZ cells (red) in control mice, but not in *Glast i⊿R3* mice. The scale bar represents 35 μm.
Student's t test: $p < 0.05$ (*); ns, not significant. Bars: mean ± SEM.
See also Figure S4.

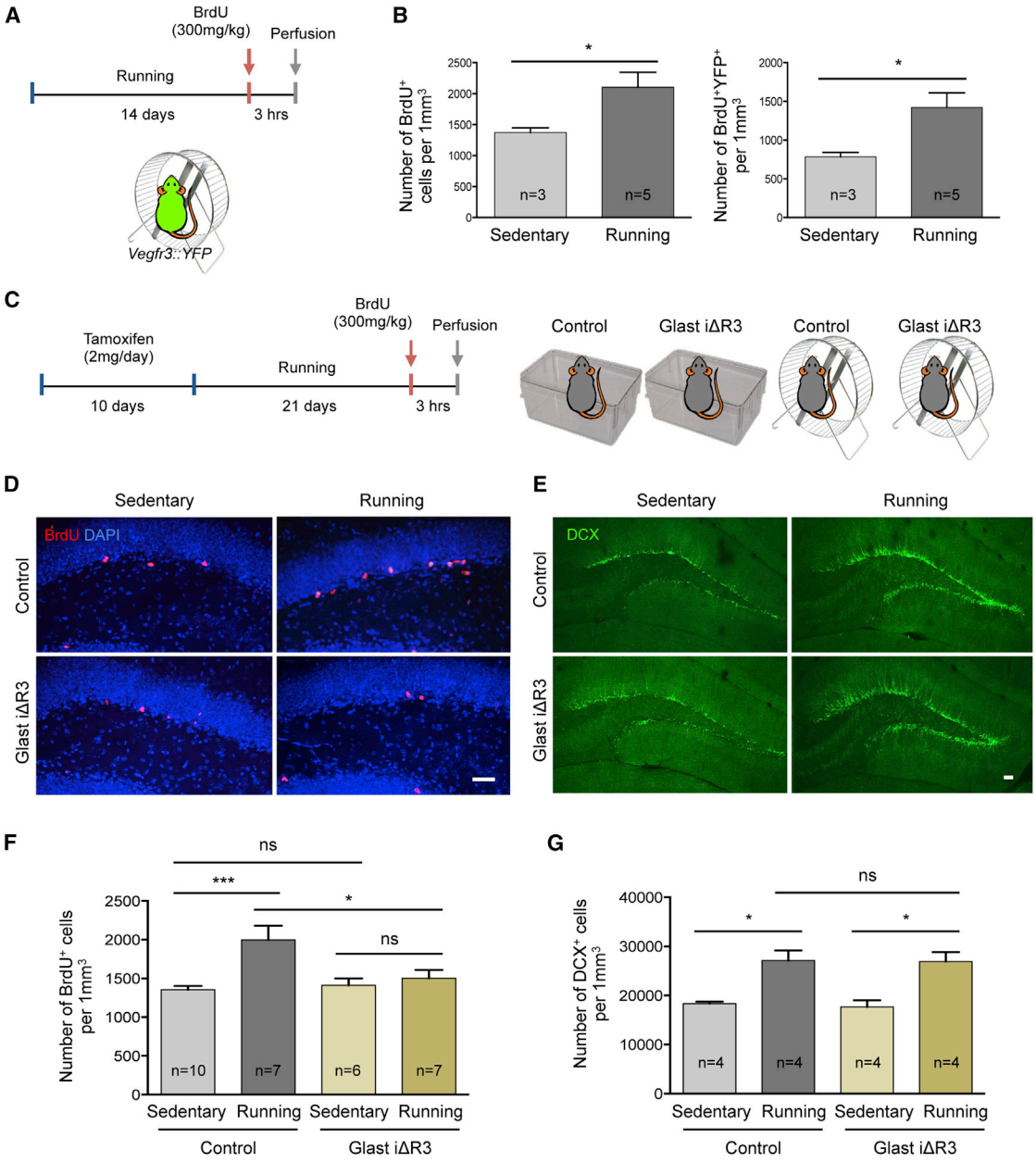

Figure 5. VEGFR3 Is Required for Exercise-Induced NSPC Proliferation

(A) Schedule of voluntary running activity and BrdU administration for *Vegfr3*::*YFP* mice.

(B) Quantification of BrdU$^+$ cells and BrdU$^+$*Vegfr3*^{YFP} cells in the SGZ of sedentary control and running *Vegfr3*::*YFP* mice.

(C) Schedule of Tx treatment, voluntary running activity, and BrdU administration in control and *Glast iΔR3* mice.

(D–G) Representative images and quantification of BrdU$^+$ SGZ cells and DCX$^+$ cells in control (upper panel) and *Glast iΔR3* mice (lower panel), either sedentary (left) or running (right). BrdU$^+$ cells (red), DAPI (blue), and DCX$^+$ cells (green) are shown. Running induces proliferation of NSCs in control mice, but not in *Glast iΔR3* mice. A similar number of neuroblasts is generated in control and *Glast iΔR3* mice. The scale bar represents 35 μm.

Student's t test: $p < 0.05$ (*); $p < 0.001$ (***); not significant (ns). Bars: mean ± SEM.

See also Figure S5.

and multiplying this number of cells by the number of serial sections (number of cells/series × 6). Total volume was determined by summing the traced DG areas for each section multiplied by the distance between sections sampled (area × 240 μm). To calculate the number of marker$^+$ cells per volume (1 mm^3), the total number of marker$^+$ cells was divided by the total volume.

hESC-Derived NSC Cultures

We have progressively differentiated hESCs into free-floating SNMs that contain self-renewing, multipotent NSCs according to a protocol (Cho et al., 2008). All experiments have been performed on SNMs derived from two different H1 (male) and H9 (female) hESC lines (Allegrucci and Young, 2007). Detailed information is provided in Supplemental Experimental Procedures.

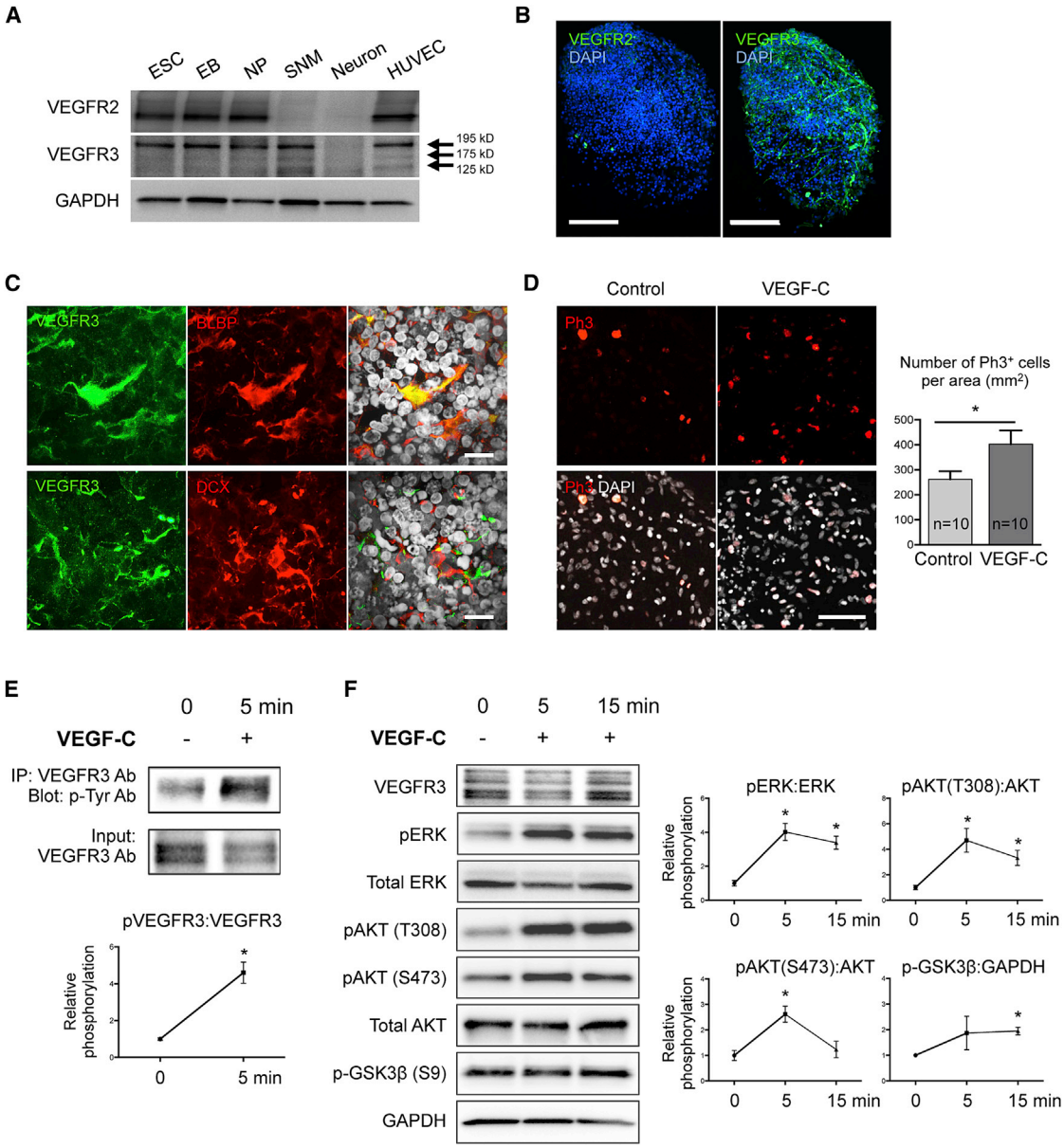

Figure 6. VEGFR3-Signaling Pathway in Human NSCs

(A) Western blot analysis of VEGFR2 and VEGFR3 expression in H1 human-ESC-derived NSCs. *VEGFR3* migrates as *three molecular weight* species: 195, 175, and 125 kDa (arrows). EB, embryoid bodies; ESC, embryonic stem cells; HUVEC, human umbilical vein endothelial cells; NP, neural progenitors; SNM, spherical neural mass.

(B) SNMs stained with anti-hVEGFR2 and -hVEGFR3 antibodies as indicated. The scale bars represent 100 μm.

(C) SNMs stained for VEGFR3 (green), BLBP (red; astroglia/NSC), or DCX (red; neuron) and DAPI (gray). The scale bars represent 20 μm.

(D) Representative image of phospho-histone H3 staining. The scale bar represents 100 μm.

(E) Phospo-VEGFR3 analysis by immunoprecipitation.

(F) Western blot analysis of the phosphorylation state of ERK, AKT (tyrosine 398 and serine 473), and GSK3β in SNMs after VEGF-C stimulation.

Student's t test: $p < 0.05$ (*). Bars/lines: mean ± SEM.

See also Figure S6.

Statistics

A two-tailed, unpaired Student's t test or Mann-Whitney test were done to determine statistical significance (Graph-Pad Prism 6). Differences were considered statistically significant if the p value was 0.05 (*$p < 0.05$; **$p < 0.01$; ***$p < 0.005$). Error estimates were displayed as SEM.

ACCESSION NUMBERS

According to the MIAME guidelines, all transcriptomic data were submitted to a MIAME compliant repository, NCBI's Gene Expression Omnibus (GEO), and are accessible through the GEO accession number GSE55621.

SUPPLEMENTAL INFORMATION

Supplemental Information includes Supplemental Experimental Procedures, six figures, and two tables and can be found with this article online at http://dx.doi.org/10.1016/j.celrep.2015.01.049.

AUTHOR CONTRIBUTIONS

J.H. contributed to the in vivo studies and manuscript; C.-F.C. and M.L. contributed to the in vitro studies; K.L.B. contributed to the in vivo studies; T.H.K. contributed to the RNA-seq analysis and hNSC studies; J.-H.P. and C.P. contributed to the immunostaining; H.N. and K.L.B. contributed the AAVs and mice; R.S.D. contributed methodological advice and practical support for behavior studies; A.C.E. contributed to the research design and manuscript; and J.-L.T. contributed to the research design and manuscript.

ACKNOWLEDGMENTS

This work was supported by Institut National de la Sante et de la Recherche Medicale (to J.-L.T.), Agence Nationale Recherche (10-BLANC-1412-01 and 13-BSV4-0002-01; to J.-L.T.), Carnot Maturation (to J.-L.T.), Leducq Foundation Transatlantic Network of Excellence (ARTEMIS; to A.C.E.), NIH (1R01EB016629-01A1 to J.-L.T. and 1R01HL111504-01 to A.C.E.), and Connecticut Stem Cell Research Fund (13-SCA-Yale-04; to J.-L.T.). We acknowledge Hongjun Song and Gregrory Enikolopov for stimulating discussion; Neil Fournier and Mounira Banasr for assistance and technical advice for behavior tests; Andrey Anisimov and the AAV Gene Transfer and Cell Therapy Core Facility of Biomedicum Helsinki, University of Helsinki, for providing us AAV-expression vectors; and Catherine Blanc (Flow Cytometry Core of Pitié-Salpétrière Hospital) for technical help.

Received: March 5, 2014
Revised: December 12, 2014
Accepted: January 20, 2015
Published: February 19, 2015

REFERENCES

Ables, J.L., Decarolis, N.A., Johnson, M.A., Rivera, P.D., Gao, Z., Cooper, D.C., Radtke, F., Hsieh, J., and Eisch, A.J. (2010). Notch1 is required for maintenance of the reservoir of adult hippocampal stem cells. J. Neurosci. *30*, 10484–10492.

Abrajano, J.J., Qureshi, I.A., Gokhan, S., Molero, A.E., Zheng, D., Bergman, A., and Mehler, M.F. (2010). Corepressor for element-1-silencing transcription factor preferentially mediates gene networks underlying neural stem cell fate decisions. Proc. Natl. Acad. Sci. USA *107*, 16685–16690.

Aguirre, A., Rubio, M.E., and Gallo, V. (2010). Notch and EGFR pathway interaction regulates neural stem cell number and self-renewal. Nature *467*, 323–327.

Allegrucci, C., and Young, L.E. (2007). Differences between human embryonic stem cell lines. Hum. Reprod. Update *13*, 103–120.

Altman, J., and Das, G.D. (1965). Autoradiographic and histological evidence of postnatal hippocampal neurogenesis in rats. J. Comp. Neurol. *124*, 319–335.

Andersen, J., Urbán, N., Achimastou, A., Ito, A., Simic, M., Ullom, K., Martynoga, B., Lebel, M., Göritz, C., Frisén, J., et al. (2014). A transcriptional mechanism integrating inputs from extracellular signals to activate hippocampal stem cells. Neuron *83*, 1085–1097.

Benedito, R., Rocha, S.F., Woeste, M., Zamykal, M., Radtke, F., Casanovas, O., Duarte, A., Pytowski, B., and Adams, R.H. (2012). Notch-dependent VEGFR3 upregulation allows angiogenesis without VEGF-VEGFR2 signalling. Nature *484*, 110–114.

Bonaguidi, M.A., Wheeler, M.A., Shapiro, J.S., Stadel, R.P., Sun, G.J., Ming, G.L., and Song, H. (2011). In vivo clonal analysis reveals self-renewing and multipotent adult neural stem cell characteristics. Cell *145*, 1142–1155.

Bonaguidi, M.A., Song, J., Ming, G.L., and Song, H. (2012). A unifying hypothesis on mammalian neural stem cell properties in the adult hippocampus. Curr. Opin. Neurobiol. *22*, 754–761.

Bordey, A. (2014). Endogenous stem cells for enhancing cognition in the diseased brain. Front. Neurosci. *8*, 98.

Brown, J., Cooper-Kuhn, C.M., Kempermann, G., Van Praag, H., Winkler, J., Gage, F.H., and Kuhn, H.G. (2003). Enriched environment and physical activity stimulate hippocampal but not olfactory bulb neurogenesis. Eur. J. Neurosci. *17*, 2042–2046.

Calvo, C.F., Fontaine, R.H., Soueid, J., Tammela, T., Makinen, T., Alfaro-Cervello, C., Bonnaud, F., Miguez, A., Benhaim, L., Xu, Y., et al. (2011). Vascular endothelial growth factor receptor 3 directly regulates murine neurogenesis. Genes Dev. *25*, 831–844.

Canteras, N.S., Resstel, L.B., Bertoglio, L.J., Carobrez, Ade.P., and Guimarães, F.S. (2010). Neuroanatomy of anxiety. Curr. Top. Behav. Neurosci. *2*, 77–96.

Cho, M.S., Hwang, D.Y., and Kim, D.W. (2008). Efficient derivation of functional dopaminergic neurons from human embryonic stem cells on a large scale. Nat. Protoc. *3*, 1888–1894.

DeCarolis, N.A., Mechanic, M., Petrik, D., Carlton, A., Ables, J.L., Malhotra, S., Bachoo, R., Götz, M., Lagace, D.C., and Eisch, A.J. (2013). In vivo contribution of nestin- and GLAST-lineage cells to adult hippocampal neurogenesis. Hippocampus *23*, 708–719.

Doetsch, F., Caillé, I., Lim, D.A., García-Verdugo, J.M., and Alvarez-Buylla, A. (1999). Subventricular zone astrocytes are neural stem cells in the adult mammalian brain. Cell *97*, 703–716.

Dranovsky, A., Picchini, A.M., Moadel, T., Sisti, A.C., Yamada, A., Kimura, S., Leonardo, E.D., and Hen, R. (2011). Experience dictates stem cell fate in the adult hippocampus. Neuron *70*, 908–923.

During, M.J., and Cao, L. (2006). VEGF, a mediator of the effect of experience on hippocampal neurogenesis. Curr. Alzheimer Res. *3*, 29–33.

Ehm, O., Göritz, C., Covic, M., Schäffner, I., Schwarz, T.J., Karaca, E., Kempkes, B., Kremmer, E., Pfrieger, F.W., Espinosa, L., et al. (2010). RBPJkappa-dependent signaling is essential for long-term maintenance of neural stem cells in the adult hippocampus. J. Neurosci. *30*, 13794–13807.

Eichmann, A., and Thomas, J.L. (2013). Molecular parallels between neural and vascular development. Cold Spring Harb. Perspect. Med. *3*, a006551.

Eisch, A.J., and Petrik, D. (2012). Depression and hippocampal neurogenesis: a road to remission? Science *338*, 72–75.

Encinas, J.M., and Sierra, A. (2012). Neural stem cell deforestation as the main force driving the age-related decline in adult hippocampal neurogenesis. Behav. Brain Res. *227*, 433–439.

Encinas, J.M., Vaahtokari, A., and Enikolopov, G. (2006). Fluoxetine targets early progenitor cells in the adult brain. Proc. Natl. Acad. Sci. USA *103*, 8233–8238.

Encinas, J.M., Michurina, T.V., Peunova, N., Park, J.H., Tordo, J., Peterson, D.A., Fishell, G., Koulakov, A., and Enikolopov, G. (2011). Division-coupled astrocytic differentiation and age-related depletion of neural stem cells in the adult hippocampus. Cell Stem Cell *8*, 566–579.

Fasano, C.A., Phoenix, T.N., Kokovay, E., Lowry, N., Elkabetz, Y., Dimos, J.T., Lemischka, I.R., Studer, L., and Temple, S. (2009). Bmi-1 cooperates with Foxg1 to maintain neural stem cell self-renewal in the forebrain. Genes Dev. *23*, 561–574.

Fournier, N.M., and Duman, R.S. (2012). Role of vascular endothelial growth factor in adult hippocampal neurogenesis: implications for the pathophysiology and treatment of depression. Behav. Brain Res. *227*, 440–449.

Gaál, E.I., Tammela, T., Anisimov, A., Marbacher, S., Honkanen, P., Zarkada, G., Leppänen, V.M., Tatlisumak, T., Hernesniemi, J., Niemelä, M., and Alitalo, K. (2013). Comparison of vascular growth factors in the murine brain reveals placenta growth factor as prime candidate for CNS revascularization. Blood *122*, 658–665.

Gao, Z., Ure, K., Ding, P., Nashaat, M., Yuan, L., Ma, J., Hammer, R.E., and Hsieh, J. (2011). The master negative regulator REST/NRSF controls adult

neurogenesis by restraining the neurogenic program in quiescent stem cells. J. Neurosci. *31*, 9772–9786.

Gould, T.D., Dao, D.T., and Kovacsics, C.E. (2009). The open field test. In Mood and Anxiety Related Phenotypes in Mice, T.D. Gould, ed. (Springer), pp. 1–20.

Gross, C., Zhuang, X., Stark, K., Ramboz, S., Oosting, R., Kirby, L., Santarelli, L., Beck, S., and Hen, R. (2002). Serotonin1A receptor acts during development to establish normal anxiety-like behaviour in the adult. Nature *416*, 396–400.

Guo, J.U., Su, Y., Shin, J.H., Shin, J., Li, H., Xie, B., Zhong, C., Hu, S., Le, T., Fan, G., et al. (2014). Distribution, recognition and regulation of non-CpG methylation in the adult mammalian brain. Nat. Neurosci. *17*, 215–222.

Haiko, P., Makinen, T., Keskitalo, S., Taipale, J., Karkkainen, M.J., Baldwin, M.E., Stacker, S.A., Achen, M.G., and Alitalo, K. (2008). Deletion of vascular endothelial growth factor C (VEGF-C) and VEGF-D is not equivalent to VEGF receptor 3 deletion in mouse embryos. Mol. Cell. Biol. *28*, 4843–4850.

Hodge, R.D., Kowalczyk, T.D., Wolf, S.A., Encinas, J.M., Rippey, C., Enikolopov, G., Kempermann, G., and Hevner, R.F. (2008). Intermediate progenitors in adult hippocampal neurogenesis: Tbr2 expression and coordinate regulation of neuronal output. J. Neurosci. *28*, 3707–3717.

Hou, Y., Shin, Y.J., Han, E.J., Choi, J.S., Park, J.M., Cha, J.H., Choi, J.Y., and Lee, M.Y. (2011). Distribution of vascular endothelial growth factor receptor-3/Flt4 mRNA in adult rat central nervous system. J. Chem. Neuroanat. *42*, 56–64.

Hur, E.M., and Zhou, F.Q. (2010). GSK3 signalling in neural development. Nat. Rev. Neurosci. *11*, 539–551.

Imayoshi, I., Shimojo, H., Sakamoto, M., Ohtsuka, T., and Kageyama, R. (2013). Genetic visualization of notch signaling in mammalian neurogenesis. Cell. Mol. Life Sci. *70*, 2045–2057.

Jang, M.H., Bonaguidi, M.A., Kitabatake, Y., Sun, J., Song, J., Kang, E., Jun, H., Zhong, C., Su, Y., Guo, J.U., et al. (2013). Secreted frizzled-related protein 3 regulates activity-dependent adult hippocampal neurogenesis. Cell Stem Cell *12*, 215–223.

Jobe, E.M., McQuate, A.L., and Zhao, X. (2012). Crosstalk among epigenetic pathways regulates neurogenesis. Front. Neurosci. *6*, 59.

Karkkainen, M.J., Haiko, P., Sainio, K., Partanen, J., Taipale, J., Petrova, T.V., Jeltsch, M., Jackson, D.G., Talikka, M., Rauvala, H., et al. (2004). Vascular endothelial growth factor C is required for sprouting of the first lymphatic vessels from embryonic veins. Nat. Immunol. *5*, 74–80.

Kempermann, G., Jessberger, S., Steiner, B., and Kronenberg, G. (2004). Milestones of neuronal development in the adult hippocampus. Trends Neurosci. *27*, 447–452.

Kim, E.J., Battiste, J., Nakagawa, Y., and Johnson, J.E. (2008). Ascl1 (Mash1) lineage cells contribute to discrete cell populations in CNS architecture. Mol. Cell. Neurosci. *38*, 595–606.

Kirkin, V., Thiele, W., Baumann, P., Mazitschek, R., Rohde, K., Fellbrich, G., Weich, H., Waltenberger, J., Giannis, A., and Sleeman, J.P. (2004). MAZ51, an indolinone that inhibits endothelial cell and tumor cell growth in vitro, suppresses tumor growth in vivo. Int. J. Cancer *112*, 986–993.

Koch, S., and Claesson-Welsh, L. (2012). Signal transduction by vascular endothelial growth factor receptors. Cold Spring Harb. Perspect. Med. *2*, a006502.

Lazarov, O., Mattson, M.P., Peterson, D.A., Pimplikar, S.W., and van Praag, H. (2010). When neurogenesis encounters aging and disease. Trends Neurosci. *33*, 569–579.

Le Bras, B., Barallobre, M.J., Homman-Ludiye, J., Ny, A., Wyns, S., Tammela, T., Haiko, P., Karkkainen, M.J., Yuan, L., Muriel, M.P., et al. (2006). VEGF-C is a trophic factor for neural progenitors in the vertebrate embryonic brain. Nat. Neurosci. *9*, 340–348.

Le Guen, L., Karpanen, T., Schulte, D., Harris, N.C., Koltowska, K., Roukens, G., Bower, N.I., van Impel, A., Stacker, S.A., Achen, M.G., et al. (2014). Ccbe1 regulates Vegfc-mediated induction of Vegfr3 signaling during embryonic lymphangiogenesis. Development *141*, 1239–1249.

Li, Y., Luikart, B.W., Birnbaum, S., Chen, J., Kwon, C.H., Kernie, S.G., Bassel-Duby, R., and Parada, L.F. (2008). TrkB regulates hippocampal neurogenesis and governs sensitivity to antidepressive treatment. Neuron *59*, 399–412.

Licht, T., and Keshet, E. (2013). Delineating multiple functions of VEGF-A in the adult brain. Cell. Mol. Life Sci. *70*, 1727–1737.

Lie, D.C., Colamarino, S.A., Song, H.J., Désiré, L., Mira, H., Consiglio, A., Lein, E.S., Jessberger, S., Lansford, H., Dearie, A.R., and Gage, F.H. (2005). Wnt signalling regulates adult hippocampal neurogenesis. Nature *437*, 1370–1375.

Lohela, M., Bry, M., Tammela, T., and Alitalo, K. (2009). VEGFs and receptors involved in angiogenesis versus lymphangiogenesis. Curr. Opin. Cell Biol. *21*, 154–165.

Lugert, S., Basak, O., Knuckles, P., Haussler, U., Fabel, K., Götz, M., Haas, C.A., Kempermann, G., Taylor, V., and Giachino, C. (2010). Quiescent and active hippocampal neural stem cells with distinct morphologies respond selectively to physiological and pathological stimuli and aging. Cell Stem Cell *6*, 445–456.

Lugert, S., Vogt, M., Tchorz, J.S., Müller, M., Giachino, C., and Taylor, V. (2012). Homeostatic neurogenesis in the adult hippocampus does not involve amplification of Ascl1(high) intermediate progenitors. Nat. Commun. *3*, 670.

Machold, R., Hayashi, S., Rutlin, M., Muzumdar, M.D., Nery, S., Corbin, J.G., Gritli-Linde, A., Dellovade, T., Porter, J.A., Rubin, L.L., et al. (2003). Sonic hedgehog is required for progenitor cell maintenance in telencephalic stem cell niches. Neuron *39*, 937–950.

Matsuda, S., Kuwako, K., Okano, H.J., Tsutsumi, S., Aburatani, H., Saga, Y., Matsuzaki, Y., Akaike, A., Sugimoto, H., and Okano, H. (2012). Sox21 promotes hippocampal adult neurogenesis via the transcriptional repression of the Hes5 gene. J. Neurosci. *32*, 12543–12557.

Mira, H., Andreu, Z., Suh, H., Lie, D.C., Jessberger, S., Consiglio, A., San Emeterio, J., Hortigüela, R., Marqués-Torrejón, M.A., Nakashima, K., et al. (2010). Signaling through BMPR-IA regulates quiescence and long-term activity of neural stem cells in the adult hippocampus. Cell Stem Cell *7*, 78–89.

Mori, T., Tanaka, K., Buffo, A., Wurst, W., Kühn, R., and Götz, M. (2006). Inducible gene deletion in astroglia and radial glia—a valuable tool for functional and lineage analysis. Glia *54*, 21–34.

Mu, Y., and Gage, F.H. (2011). Adult hippocampal neurogenesis and its role in Alzheimer's disease. Mol. Neurodegener. *6*, 85.

Okano, H., Kawahara, H., Toriya, M., Nakao, K., Shibata, S., and Imai, T. (2005). Function of RNA-binding protein Musashi-1 in stem cells. Exp. Cell Res. *306*, 349–356.

Pellow, S., Chopin, P., File, S.E., and Briley, M. (1985). Validation of open: closed arm entries in an elevated plus-maze as a measure of anxiety in the rat. J. Neurosci. Methods *14*, 149–167.

Petersen, P.H., Zou, K., Hwang, J.K., Jan, Y.N., and Zhong, W. (2002). Progenitor cell maintenance requires numb and numblike during mouse neurogenesis. Nature *419*, 929–934.

Phoenix, T.N., and Temple, S. (2010). Spred1, a negative regulator of Ras-MAPK-ERK, is enriched in CNS germinal zones, dampens NSC proliferation, and maintains ventricular zone structure. Genes Dev. *24*, 45–56.

Quentmeier, H., Eberth, S., Romani, J., Weich, H.A., Zaborski, M., and Drexler, H.G. (2012). DNA methylation regulates expression of VEGF-R2 (KDR) and VEGF-R3 (FLT4). BMC Cancer *12*, 19.

Robins, S.C., Stewart, I., McNay, D.E., Taylor, V., Giachino, C., Goetz, M., Ninkovic, J., Briancon, N., Maratos-Flier, E., Flier, J.S., et al. (2013). α-Tanycytes of the adult hypothalamic third ventricle include distinct populations of FGF-responsive neural progenitors. Nat. Commun. *4*, 2049.

Saharan, S., Jhaveri, D.J., and Bartlett, P.F. (2013). SIRT1 regulates the neurogenic potential of neural precursors in the adult subventricular zone and hippocampus. J. Neurosci. Res. *91*, 642–659.

Saxe, M.D., Battaglia, F., Wang, J.W., Malleret, G., David, D.J., Monckton, J.E., Garcia, A.D., Sofroniew, M.V., Kandel, E.R., Santarelli, L., et al. (2006). Ablation of hippocampal neurogenesis impairs contextual fear conditioning and synaptic plasticity in the dentate gyrus. Proc. Natl. Acad. Sci. USA *103*, 17501–17506.

Snyder, J.S., Soumier, A., Brewer, M., Pickel, J., and Cameron, H.A. (2011). Adult hippocampal neurogenesis buffers stress responses and depressive behaviour. Nature *476*, 458–461.

Suh, H., Consiglio, A., Ray, J., Sawai, T., D'Amour, K.A., and Gage, F.H. (2007). In vivo fate analysis reveals the multipotent and self-renewal capacities of Sox2+ neural stem cells in the adult hippocampus. Cell Stem Cell *1*, 515–528.

Tammela, T., Zarkada, G., Wallgard, E., Murtomäki, A., Suchting, S., Wirzenius, M., Waltari, M., Hellström, M., Schomber, T., Peltonen, R., et al. (2008). Blocking VEGFR-3 suppresses angiogenic sprouting and vascular network formation. Nature *454*, 656–660.

Tammela, T., Zarkada, G., Nurmi, H., Jakobsson, L., Heinolainen, K., Tvorogov, D., Zheng, W., Franco, C.A., Murtomäki, A., Aranda, E., et al. (2011). VEGFR-3 controls tip to stalk conversion at vessel fusion sites by reinforcing Notch signalling. Nat. Cell Biol. *13*, 1202–1213.

van Wijngaarden, P., and Franklin, R.J. (2013). Ageing stem and progenitor cells: implications for rejuvenation of the central nervous system. Development *140*, 2562–2575.

Vivar, C., and van Praag, H. (2013). Functional circuits of new neurons in the dentate gyrus. Front. Neural Circuits *7*, 15.

Zacchigna, S., Lambrechts, D., and Carmeliet, P. (2008). Neurovascular signalling defects in neurodegeneration. Nat. Rev. Neurosci. *9*, 169–181.